Motions of a swinging Atwood's machine

N. Tufillaro

Classification
Physics Abstracts
02.30 — 03.20

Motions of a Swinging Atwood's Machine

N. Tufillaro

Physics Department, Bryn Mawr College, Bryn Mawr, Pennsylvania 19010, U.S.A.

Résumé. — Le lagrangien

$$L_\mu(r, \theta) = \tfrac{1}{2}(1 + \mu)\, \dot{r}^2 + \tfrac{1}{2}\, r^2\, \dot{\theta}^2 - r(\mu - \cos\theta)$$

avec $1 < \mu \leqslant 3,1$ est étudié en utilisant une section de Poincaré. Les résultats numériques suggèrent que le système est intégrable pour $\mu = 3$. Nous démontrons l'intégrabilité en explicitant une intégrale première du mouvement.

Abstract. — The Lagrangian

$$L_\mu(r, \theta) = \tfrac{1}{2}(1 + \mu)\, \dot{r}^2 + \tfrac{1}{2}\, r^2\, \dot{\theta}^2 - r(\mu - \cos\theta)$$

with $1 < \mu \leqslant 3.1$ is studied using a surface of section map. Regular and chaotic behaviour is exhibited. The numerical evidence suggests the motion is integrable for $\mu = 3$. Integrability is proved by explicitly exhibiting a first integral.

1. Introduction.

A conservative dynamical system depending on a parameter μ with Lagrangian $(L_\mu = T_\mu - V_\mu)$ of the form

$$T_\mu(r, \theta) = \frac{1}{2}(1 + \mu)\, \dot{r}^2 + \frac{1}{2}r^2\, \dot{\theta}^2, \qquad (1)$$

$$V_\mu(r, \theta) = r(\mu - \cos\theta), \qquad (2)$$

arises in a Swinging Atwood's Machine (SAM) [1]. This is an ordinary Atwood's Machine, in which however, one of the weights can swing in a plane (Fig. 1). The constant μ is the mass ratio of the non-swinging to the swinging weight. Perturbative techniques are used to study the periodic orbits of SAM in reference [1]. Therein a remarkable property is discovered; if $\mu = 3$ then any trajectory that begins at the origin will execute a symmetrical loop and return to the origin no matter what the launch angle or speed (see Fig. 2).

In this study the global dynamics of SAM are explored by numerically constructing surface of section (SOS) maps for various values of μ. This method of investigation originated with Poincaré and is explained by Berry and others [2, 3]. The evolution of the global dynamics are observed as μ varies from one to three.
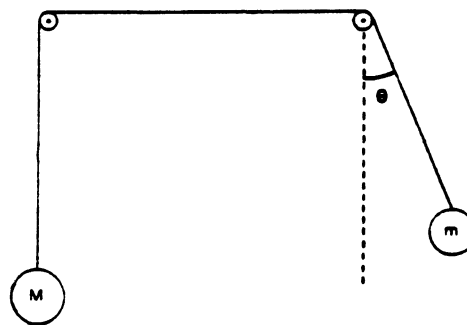
Fig. 1. — <u>Swinging Atwood's Machine. The mass ratio $\mu = M/m$.</u>

The qualitative picture that emerges suggests the motion is integrable when $\mu = 3$. Integrability is proved by finding a second invariant that is quadratic in the velocities.

Examples of integrable mechanical systems with two-degrees of freedom are still rare. Known cases include Newtonian force under two-fixed centres, and all central force problems. SAM is a very simple mechanical system that exhibits a great richness of behaviour. That such a simple system is integrable for some parameter values is surprising. A greater
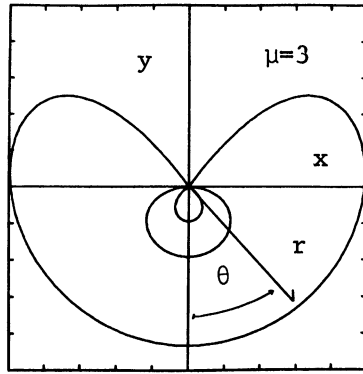
Fig. 2. — Ejection/collision trajectors for SAM. When $\mu = 3$ all trajectories that are fired from the origin execute a symmetrical loop and return to the origin. Three different such trajectories are shown.

understanding of how this occurs would be useful in the analysis of other parameter dependent Hamiltonian systems.

2. Dynamics.

2.1 GENERALITIES. — The potential V_μ is a homogeneous function of degree one. Thus the principle of mechanical similarity applies [4]; the orbits on a given energy surface can be rescaled to orbits at any other energy. *The dynamics generated by V_μ are independent of the energy constant.* Throughout this study set $E = 1$ without loss of generality.

The velocity of the swinging mass is zero at

$$r_\mu(\theta) = \frac{1}{\mu - \cos(\theta)},\qquad (3)$$

which defines the *zero-velocity* curve. If $\mu > 1$ then equation (3) is an ellipse with one focus at the origin and eccentricity $1/\mu$. Because $T_\mu \geqslant 0$, the trajectories are bounded by,

$$r_{max} \leqslant \frac{1}{\mu - \cos \theta},\qquad \mu > 1,\qquad (4)$$

the zero-velocity ellipse.

Furthermore the system is symmetric about the vertical y-axis (Fig. 2). Thus an orbit will be periodic if any of the events below occurs twice in any combination :

(i) the orbit is perpendicular to an axis of symmetry ;
(ii) the orbit reaches the zero-velocity curve.

In the latter case a periodic orbit is called an *oscillation*, otherwise it is known as a *rotation*. The simplest oscillation has been dubbed a *smile* (Fig. 3a) [5]. *Loops* (Fig. 3b) and smiles will play an important role in what follows.

Lastly, the equations of motion

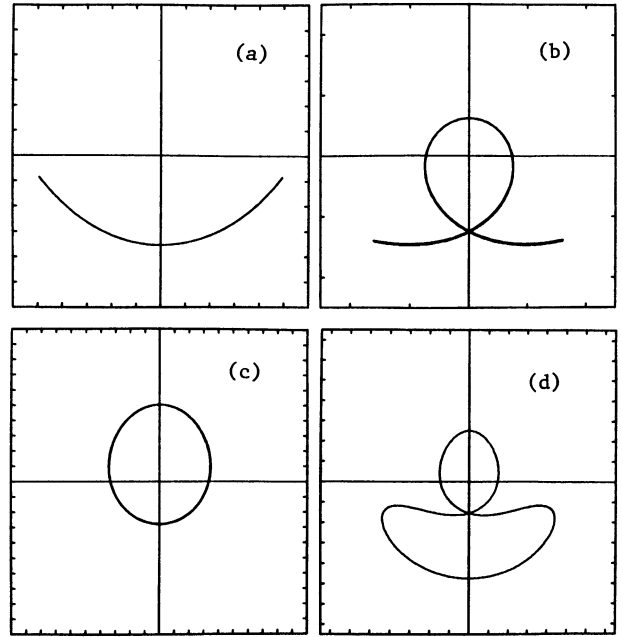$$(1 + \mu)\,\ddot{r} = r\dot{\theta}^2 + (\cos \theta - \mu),\qquad (5)$$

Fig. 3. — Periodic orbits. Examples of oscillations are : (a) smile, (b) loop. Examples of rotations are : (c) egg, (d) weeble. The initial conditions — $(r_0, \theta_0, \dot{r}_0, \dot{\theta}_0, \mu)$ — are : (a) (1, 1.4, 0, 0, 1.527); (b) (0.25, 0.35, 0, 2.83, 3); (c) (1, 0, π, 1, 4.35); (d) (0.5, 0, π, 1, 1.95).

$$r\ddot{\theta} + 2\,\dot{r}\dot{\theta} + \sin \theta = 0,\qquad (6)$$

are singular at the origin. The acceleration is discontinuous at $r = 0$. Trajectories starting at the origin are called *ejections*. Those arriving are termed *collisions*. For $\mu = 3$ all ejections end in collisions. In the region $r/r_{max} \ll 1$ an approximate solution to equations (5) and (6) is [1] :

$$r(\theta) = \frac{A}{\cos\left(\dfrac{\theta - \theta_1}{\sqrt{1 + \mu}}\right)},\qquad (7)$$

where θ_1 is the angle of closest approach. This motivates the extension of ejection/collision orbits through the origin by the rule :

$$(r, \theta, \dot{r}, \dot{\theta}) \to (r, \bar{\theta}, -\dot{r}, \dot{\theta}),\qquad (8)$$

$$\bar{\theta} = \pi\sqrt{1 + \mu} + \theta.\qquad (9)$$

Note that $\theta = \bar{\theta}$ for $\mu = 4n^2 - 1 = 3, 15, 35...$

2.2 SURFACE OF SECTION MAP. — Consider the state space $(r, \theta, \dot{r}, \dot{\theta})$. The global dynamics of SAM may be viewed *via* a SOS map defined as follows. With $E = 1$ solve $E = T_\mu + V_\mu$ for $\dot{\theta}$. Now set $\theta = 0$ to get

$$\dot{\theta}(r, \dot{r}) = \pm \frac{\sqrt{2}}{r}\left\{ 1 + (1 - \mu)\,r - \frac{1}{2}(1 + \mu)\,\dot{r}^2 \right\}^{1/2}.\qquad (10)$$

The SOS consists of all points $(r, \dot{r})$ such that $\dot{\theta}$ is real. The boundary of the SOS $(\dot{\theta} = 0)$ is a parabola. Every point on this SOS corresponds to a trajectory of SAM. The equations of motion repeatedly map this SOS onto itself. To see that this map is well defined we must check that : (a) every orbit crosses the $\theta = 0$ axis, and (b) the map is continuous. Property (a) is obvious [6], while (b) is true if we include the extension (Eq. (8)) of ejection/collision orbits. Fixed points of the SOS map correspond to periodic orbits and closed curves to KAM tori [2].

The SOS map is shown in figures 4 and 5 for increasing values of μ. This map is constructed numerically by integrating [7] about 50 separate initial conditions over many cycles and computing their intersection with the SOS plane by a clever method proposed by Henon [8].

2.3 RESULTS. — The central elliptic fixed point in figure 4 (1.1) corresponds to the smile in figure 3a. This elliptic isle dominates the state space topology for $\mu = 1 + \varepsilon$, $\varepsilon \ll 1$. In this regime the dynamics are mostly regular because of the preponderance of KAM tori. As μ increases from one to three the region of stability associated with the smile decreases. However, it remains an elliptic fixed point throughout until it crashes into the singularity at $r = 0$ when $\mu = 3$. Interestingly the shape of the last KAM tori

changes as μ increases. This occurs because the fixed points surrounding the smile change from elliptic to hyperbolic and back again. For instance, figure 4(1.5) is a lovely illustration of four hyperbolic fixed points, but these unstable fixed points are not present in figures 4(1.4) or 4(1.6), and there is a corresponding change in the last KAM tori.

Not unexpectedly, irregular motion becomes more prominent as μ increases. In figure 5(2.5) most of the motion appears irregular. But in figure 5(2.8) two new elliptic isles emerge out of the sea of chaos. The new isles expand dramatically in figure 5(2.9) and correspond to the loop orbit in figure 3b. Remarkably, *in figure* 5(3.0) *the state space appears to be completely stratified by tori*; this is the hallmark of integrability and suggests that the system is integrable at $\mu = 3$. In figure 5(3.1) chaos again emerges.

Figure 5(15) also reveals no chaotic trajectories. This leads us to the somewhat more speculative conjecture that SAM is integrable when $\mu = 4n^2 - 1$, $n \in Z^+$.

3. Equivalent integrable potential

SAM's dynamics are equivalent to the motion of a particle of unit mass moving under the Cartesian potential

$$V_m(x, y) = \left\{ (2m)^{-1} - \cos^2\left[(2m^{1/2})^{-1} \arctan\left(\frac{x}{y}\right) \right] \right\} (x^2 + y^2)^{1/2}. \tag{11}$$

Equation (11) is obtained from equations (1) and (2) by the transformation :

$$m = \frac{1}{1 + \mu}, \tag{12}$$

$$x = r \sin(m^{1/2}\,\theta), \tag{13}$$

$$y = r \cos(m^{1/2}\,\theta). \tag{14}$$

For $\mu = 3$ equation (11) simplifies to

$$U(x, y) = \frac{2x^2 + y^2}{\sqrt{x^2 + y^2}}. \tag{15}$$

On converting the potential in equation (15) to parabolic coordinates

$$x = \frac{1}{2}(\xi^2 - \eta^2), \quad y = \xi\eta, \tag{16}$$

we see that $U(x, y)$ becomes

$$P(\xi, \eta) = 2\frac{\xi^4 + \eta^4}{\xi^2 + \eta^2}. \tag{17}$$

A. Ankiewicz and C. Pask [9] show that if a potential

is of the form

$$\frac{g_1(\xi) + g_2(\eta)}{\xi^2 + \eta^2}, \tag{18}$$

then the system is separable in parabolic cylinder coordinates and the second invariant is quadratic in the velocities. In our case $g_1(\xi) = \xi^4$ and $g_2(\eta) = \eta^4$. A second invariant for the potential $U(x, y)$ of equation (15) is [9]

$$C = \frac{xy^2}{\sqrt{x^2 + y^2}} - \dot{y}(x\dot{y} - y\dot{x}). \tag{19}$$

4. Conclusion.

The global dynamics of SAM are explored by means of a surface of section map. The class of periodic orbits known as smiles is shown to be stable. SAM is integrable when $\mu = 3$ and conjectured to be integrable when $\mu = 4n^2 - 1$. The integrability property may be related to the appearance of discrete symmetries in the equivalent « particle of unit mass » problem. The connection between the local singular behaviour and global integrability is currently being explored.
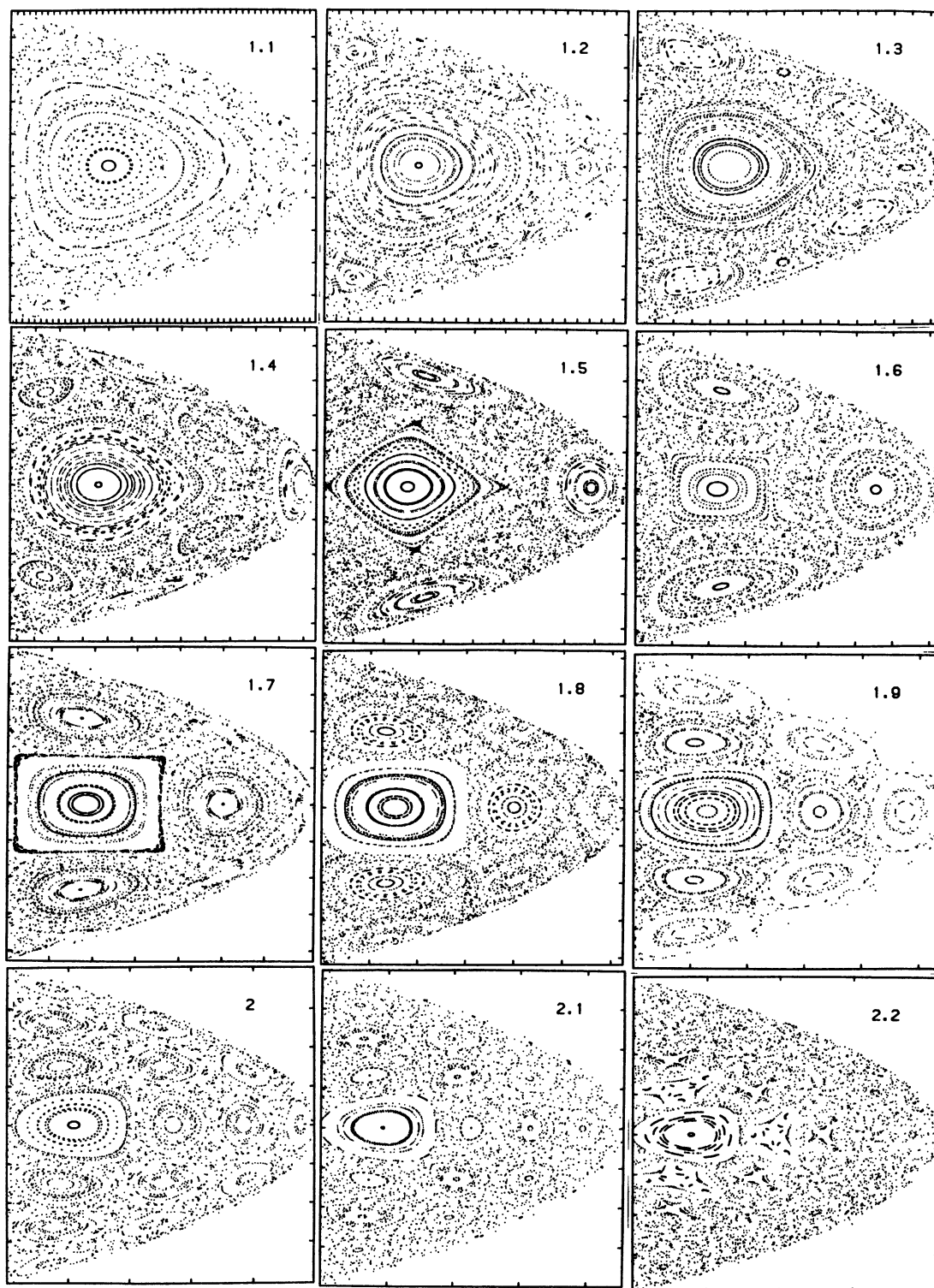
Fig. 4. — Surface of section map $(r, \dot{r})$; $1.1 \leqslant \mu \leqslant 2.2$. The value of μ is indicated in the upper right. Both regular and chaotic motion is exhibited. The central fixed point in (1.1) corresponds to the smile in figure 3a. Both the horizontal and vertical axes are scaled separately. Each tick is 0.2. The horizontal axis goes from 0 to r_{max}. The vertical axis goes from $- \dot{r}_{max}$ to $\dot{r}_{max}$.
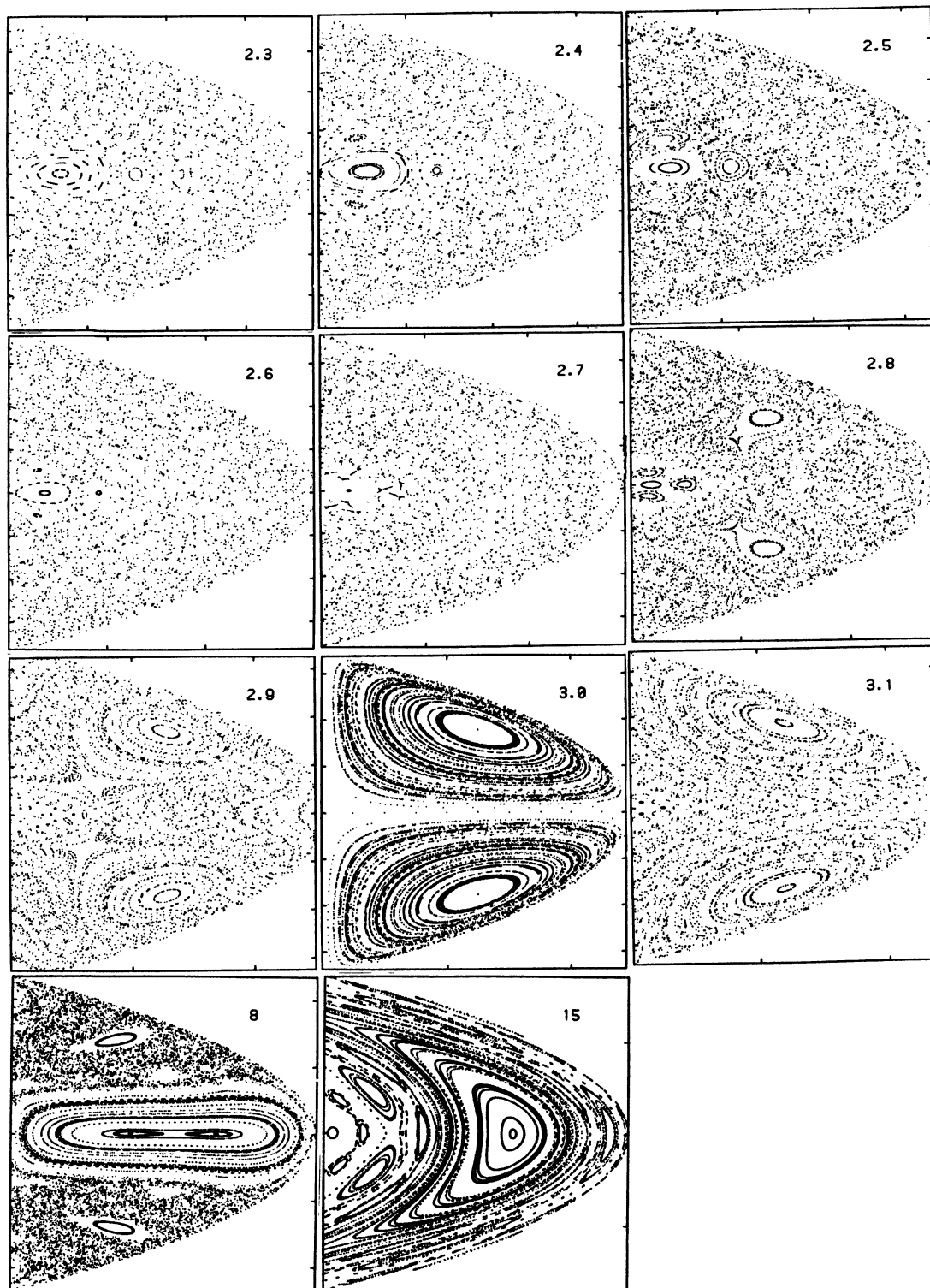
Fig. 5. — Continuation of surface of section map $(r, \dot{r})$. See figure caption 4. The motion becomes first more irregular, then more regular with the appearance of a new elliptic isle at (2.8). This elliptic fixed point corresponds to the loop in figure 3b. The loop dominates in (3.0) and the motion looks integrable.

References

[1] TUFILLARO, N. B., ABBOTT, T. A. and GRIFFITHS, D. J., Swinging Atwood's Machine, *Am. J. Phys.* (October, 1984).

[2] BERRY, M. V., Topics in Nonlinear Dynamics, *Am. Inst. Phys. Conf. Proc.* **46** (1978) 16.

[3] HENON, M. and HEILES, C., *Astron. J.* **69** (1963) 73.

[4] LANDAU, L. D. and LIFSCHITZ, E. M., *Mechanics*, Third Ed. (Pergamon, Oxford) 1976, Sect. 10.

[5] CRANDALL, R. E., *Pascal Applications for the Sciences* (Wiley, New York) 1984, p. 147.

[6] TUFILLARO, N. B., *Smiles and Teardrops*, B. A. thesis (1982), Reed College, Portland, Oregon, 97202, p. 65.

[7] TUFILLARO, N. B. and ROSS, G. A., *Ode User's Manual*, Reed College Academic Computer Center, 1981.

[8] HENON, M., *Physica* **5D** (1982) 412-414.

[9] ANKIEWICZ, A. and PASK, C., *J. Phys. A : Math. Gen.* **16** (1983) 4203-4208. (Use Eq. (19) to construct the second invariant.)